



## Scratch resistance of brittle thin films on compliant substrates

Zhong Chen<sup>a,\*</sup>, Linda Y.L. Wu<sup>b</sup>, Edmund Chwa<sup>a</sup>, Otto Tham<sup>a</sup>

<sup>a</sup> School of Materials Science and Engineering, Nanyang Technological University, 50 Nanyang Avenue, Singapore 639798, Singapore

<sup>b</sup> Singapore Institute of Manufacturing Technology, 71 Nanyang Drive, Singapore 638075, Singapore

Received 19 February 2007; received in revised form 2 July 2007; accepted 31 July 2007

### Abstract

There has been intensive interest in studying the behavior of hard and brittle thin films on compliant substrates under scratch action. The examples include sol–gel protective coatings on plastic optical lenses, safe windows, and flexible electronic devices and displays. Hard ceramic coatings have been widely used to prolong the life of cutting tools and biomedical implants. In this work, the scratch resistance of sol–gel coatings with different amount of colloidal silica on polycarbonate substrates was tested by the pencil scratch test following the ISO 15184 standard. The scratch failure was found to be tensile trailing cracking in the coating and substrate gouging. The indentation hardness, elasticity modulus and fracture toughness of the coatings were determined and correlated to the observed pencil scratch hardness. Based on the analysis, the main factors to improve the scratch resistance are the elasticity modulus, thickness and fracture toughness of the coatings. General consideration for the improvement of scratch resistance of hard coatings on compliant substrates was also discussed.

© 2007 Elsevier B.V. All rights reserved.

**Keywords:** Scratch resistance; Pencil scratch test; Hardness; Cracking; Delamination; Elastic modulus; Fracture toughness; Interfacial fracture toughness

### 1. Introduction

Hard protective coatings on compliant substrates have been widely used in applications such as plastic optical lenses, safety windows, machine tools, biomedical implants, and portable electronic displays. These coatings are often produced by physical vapour deposition [1–4], chemical vapour deposition [4–6], and sol–gel coatings [7–10]. The coating properties can be tailored by controlling the deposition parameters and coating composition according to different functional requirements. A simple and quick assessment of the quality of the coatings is by a scratching test. The test imitates the resistance to accidental damage caused by a sharp object during device usage, and can be used as a general assessment of the coating reliability. However, the disadvantage of such a simple test is that there are many factors that may affect the outcome of the test, and due to such a complexity, the current understanding is still limited. Most of the existing work is qualitative in nature; attempt in quantitative analysis is scarce. The aim of the current work is to study the scratch behavior of hard and stiff coatings produced on relatively soft and compliant substrates.

Examples used are hybrid sol–gel coatings on polycarbonate substrates. The parametric model generated from the work is semi-quantitative and applicable to other hard coating on compliant substrate systems. Such a model reveals the main factors behind scratch resistance and therefore can provide guidelines for designing scratch resistant hard coatings on compliant substrate.

Scratch is a physical action during which a sharp object is pressed onto, and drawn over the surface of the coating simultaneously. The normal load during the test is either kept constant or progressively increased. Progressively increasing scratch load eventually induces a critical point of damage such as coating delamination, coating cracking (in the case of brittle coatings) or whitening (in the case of polymeric coatings) in a single test. In the constant-load test, multiple tests at increased constant-load levels are needed in order to determine the critical scratch load. In any case, the critical load itself or its derivative (e.g. scratch hardness, defined as the load divided by indented area) is used to compare the performance of different coatings. A number of ASTM and ISO standards are available for the scratch test of coatings. ASTM C 1624 [11] describes a standard test method for hard (Vickers hardness  $HV \geq 5$  GPa) ceramic coatings, while ASTM D 7027 [12] is for the evaluation of polymeric coatings and plastics. Nano-scratch of soft coatings is described by ASTM D

\* Corresponding author.

E-mail address: aszchen@ntu.edu.sg (Z. Chen).

7187 [13]. For sol–gel coatings on polymeric substrates, pencil scratch test described by ISO 15184 [14], or its counterpart by ASTM D 3363 [15] is popularly used by the industry. Both standards were intended for the film hardness assessment of soft coatings such as paints and varnishes. But practically, they were also used on hard, protective sol–gel coatings for optical lenses, automobile topcoats and other sol–gel coatings on polymer substrates [16–19]. The pencil scratch test is a constant-load scratch test, however, it does not require increased constant-load to reach the critical point of failure. Instead, it uses pencil leads of different hardness grades as the scratch stylus, compared to the diamond stylus usually used in most other test standards. By applying the same normal load with indenters of different hardness, a critical pencil lead grade that does not cause damage to the coating is cited as the pencil hardness of the coating concerned.

## 2. Experimental details

A stock solution of 3-glycidoxypopyl trimethoxysilane (GLYMO) and tetraethylorthosilicate (TEOS) was prepared by hydrolyzing them in ethanol (EtOH) and water (H<sub>2</sub>O) in an acidic solution (HIt, itaconic acid). The molar ratios of the components were: GLYMO:TEOS:EtOH:H<sub>2</sub>O:HIt = 1.0:1.63:2.19:5.0:0.26. The GLYMO and TEOS were hydrolyzed separately and then mixed together. The mixture solution was stirred for 24 h and used as the base solution for coatings. To this base solution, a colloidal silica solution (Ludox AS-40) was first acidified by HIt to pH 3, and then added as hard filler in different molar ratios of 0.70, 2.08, 4.27, and 5.48. The colloidal silica was first coated with a monolayer of the sol–gel by adding 15 wt.% of the base solution. The purpose was to stabilize the colloidal particles to avoid flocculation when added to the sol. The adsorption of GLYMO onto colloidal silica has been studied by Daniels and Francis [20]. It was found that the maximum adsorption was limited to 2.2 monomer units/nm<sup>2</sup>. The 15 wt.% used in this study was calculated based on the maximum adsorption on the silica colloidal surface. The prevention of flocculation was observed by us during the preparation of sol–gel solution. Without the addition of GLYMO into the colloidal, the sol–gel solution turned white and never turned back to clear.

The density of the cured un-filled coating was measured to be 1.3 g/cm<sup>3</sup>, and the volume percentage of the fillers in coating matrix was calculated to be 6.7, 17.6, 30.5 and 36.0 vol.% in the cured coatings, corresponding to the different molar addition of the colloidal silica fillers. The particle size of the silica is about 20 nm, so that the coatings remained transparent after curing. Before dip coating, 0.05 wt.% of ethylenediamine (ED) was added to the coating solution as the cross-linking agent of the epoxy ring in GLYMO.

Polycarbonate (PC) substrates, measured 100 mm × 50 mm × 3 mm, were treated by oxygen plasma (MARCH PX-1000) before coating was applied. The purpose of the plasma treatment was to remove organic contaminations on the PC surface and activate the surface for better wetting and adhesion

between the coating and the substrate [21]. The treatment was done at the following conditions: RF power 400 W, pressure 130 mbar, oxygen flow rate 400 sccm, and treatment time 5 min. The pre-treated PC substrates were dip coated with the above solutions in different withdrawal speeds so that the effect of layer thickness on coating's hardness and scratch resistance could be studied. Preliminary calibration found that the coating thickness increased with the withdrawal speeds, as shown in Table 1. With increased silica concentration, the same withdrawal speed gave rise to thicker coatings. This is understandable since the viscosity increases with the filler addition.

After the dip coating, specimens were placed in a bench top furnace for drying and curing. The drying was done at 80 °C for 40 min and curing at 110 °C for 90 min. To achieve thicker coatings (>5–8 μm, depending on the colloidal concentration as shown in Table 1), varying the coating speed proved to be inadequate. Thus multiple coatings were applied. After each coating and curing step, a plasma treatment was carried out before the subsequent layer was applied. This is to avoid mixing of the two layers and to eliminate potential risk of cracking upon curing.

The final thickness of the coating was measured using a profilometer (Talysurf Series 2 Stylus Profilometer) across the uncoated and coated areas on the same specimen. The scratch resistance of the coating was characterized by a commercial pencil hardness tester (Scratch Hardness Tester Model 291, Erichsen Testing Equipment, Germany). The test conformed to the ISO standard 15184 [14], where a vertical force of  $7.5 \pm 0.1$  N was applied at tip of the pencil. The pencil was fixed at 45° angle to the horizontal coating surface as the pencil was moved over the coated specimen. The pencil lead was flattened before the test as specified in the standard. From soft to hard (9B to 9H), the hardest pencil grade that does not cause damage to the coated specimen was termed as the pencil hardness of the coating. We have added a measurement of the tangential force during the pencil scratch test. Effective friction coefficient was given as quotient of the steady-state tangential force over the vertical force. The term “effective friction coefficient” was used to take into account the change of the film surface condition during the test. Therefore it was expected that film damage (e.g. cracking, delamination) would cause an increase in the effective friction coefficient. On the other hand, by the conventional definition, the friction coefficient between a pencil/film friction pair should have a fixed value.

The intrinsic hardness (referred to as indentation hardness thereafter) and Young's modulus of the coatings were measured using a nano-indenter (NanoTest<sup>TM</sup>, Micro Materials Limited, Wrexham, United Kingdom). The nano-indentation was carried in the depth-controlled mode, with depth of the indentation controlled at around 850 nm for all cases. To measure the film fracture toughness, coatings were applied on thinner PC substrates of 200-μm thick and tested by the controlled buckling test method, which was described elsewhere [22–24]. 8–10 samples were tested for each type of coatings. The residual stress caused by curing shrinkage was measured by the curvature method [25] and was taken into consideration in the fracture toughness calculation.

Table 1  
Coating thickness at different withdrawal speeds for coatings with different colloidal content

Withdrawal speed (cm/min)	Colloidal silica content (vol.%)														
	0.0			6.7			17.6			30.5			36.0		
	Thickness ( $\mu\text{m}$ )	Pencil grade	Thickness ( $\mu\text{m}$ )	Pencil grade	Thickness ( $\mu\text{m}$ )	Pencil grade	Thickness ( $\mu\text{m}$ )	Pencil grade	Thickness ( $\mu\text{m}$ )	Pencil grade	Thickness ( $\mu\text{m}$ )	Pencil grade	Thickness ( $\mu\text{m}$ )	Pencil grade	
12.7	1.5	2B	2.5	2B	2.8	2B	3.8	HB	5.2	F	5.2	H	5.2	H	
25.4	2.3	2B	3.1	B	3.2	B	5.5	F	6.3	H	6.3	H	6.3	H	
38.1	2.9	2B	3.2	B	4.6	B	7.4	F	7.3	2H	7.3	2H	7.3	2H	
50.8	3.0	2B	3.9	B	6.5	B	7.6	F	7.5	2H	7.5	2H	7.5	2H	
63.5	3.5	2B	4.2	B	6.8	B	7.7	H	7.9	2H	7.9	2H	7.9	2H	
76.2	4.7	B	4.6	B	7.1	B	7.9	H	8.3	2H	8.3	2H	8.3	2H	
88.9	4.9	B	5.2	HB	7.7	HB	8.2	H	8.5	2H	8.5	2H	8.5	2H	

Pencil hardness grade is also shown in the table.

### 3. Results and analysis

From Table 1, it is clear that with increasing withdrawal speed, the coating thickness increases, and the pencil hardness increases too for coatings with the same silica volume fraction. The general trend was observed that coatings with higher silica addition possessed higher pencil grades. However, for single layer coating, the increase was limited, as the highest pencil grade achieved was only 2H. For quite a number of industrial applications, a minimum of 4–5 H is required.

Table 2 shows the indentation hardness, Young's modulus, and the scratch pencil hardness of coatings with different colloidal silica content on specimens with approximately the same coating thickness (within the range of  $5 \pm 0.5 \mu\text{m}$ ). In such a comparison, the influence of the coating thickness was minimized. The residual stress after curing and the fracture toughness were also reported in the same table. The results show that indentation hardness and modulus increased with the silica content. The increase in hardness and elastic modulus is easily understandable since the added silica is harder and stiffer than the matrix. The nano-indentation hardness and pencil hardness of the PC substrate without coating were 0.19 GPa and 6B, respectively.

There was a mild increase in coating fracture toughness with silica content. With more colloidal silica added, the coating becomes harder and stiffer, and usually the ability to absorb energy tends to decrease. However, in the case of sol–gel coatings, the beneficial effect with increased colloidal silica content could be explained by the difference in porosity. Sol–gel coatings usually possess lots of pores after curing. Coatings with more colloidal silica added have a lower residual porosity due to the filling of the pores and the chemical bonding of the silica nano-particles with the sol–gel matrix. Therefore, the pores in these coatings will be smaller than the ones in the coatings with less colloidal silica. The pores in brittle coatings act as flaws causing stress concentration; and the larger the flaw size, the lower the coating fracture resistance. This analysis can be justified by the report of Nogami and Moriya [26] in which the full strength and density of the silica sol–gel could only be obtained by heating at 700 °C or above. In the current work, the sol–gel coating was cured at 120 °C due to the limited heat resistance of the PC substrate. Therefore, pores in the coatings are inevitable, and hydroxyl groups are trapped on the surface of the pores [20]. Since the colloidal silica surface is terminated by –OH groups, which can react with the –OH groups on pore surface and within the sol–gel matrix to form chemical bond, the addition of colloidal silica would help to reduce the pores and enhance the chemical bonding within the coating material.

The residual stress (Table 2) is tensile (positive values) for all five types of coatings. There is a slight decrease with the increase of colloidal concentration, which suggests that silica filler tends to reduce the curing shrinkage. This agrees with the pore–silica interaction argument made above. The magnitude of the stress is relatively low (e.g. compared to the compressive yield strength), therefore it is not expected to affect the measured indentation hardness and elasticity modulus significantly. However, it can exert a considerable impact on the coating cracking.

Table 2

Pencil hardness, indentation hardness, Young's modulus, residual stress and fracture toughness of coatings with different silica content

	Colloidal silica content (vol.%)				
	0.0	6.7	17.6	30.5	36.0
Pencil hardness grade	B	HB	F	H	H
Indentation hardness (GPa)	$0.59 \pm 0.003$	$0.62 \pm 0.013$	$0.66 \pm 0.022$	$0.71 \pm 0.029$	$0.88 \pm 0.032$
Young's modulus (GPa)	$2.65 \pm 0.02$	$5.26 \pm 0.05$	$5.43 \pm 0.06$	$8.30 \pm 0.15$	$9.99 \pm 0.19$
Coating thickness ( $\mu\text{m}$ )	4.9	5.2	4.6	5.5	5.2
Residual stress (MPa)	$31.5 \pm 9.6$	$26.6 \pm 6.0$	$25.6 \pm 8.7$	$23.0 \pm 1.2$	$23.4 \pm 12.0$
Fracture toughness ( $\text{J/m}^2$ )	$8.5 \pm 3.3$	$8.5 \pm 1.7$	$8.7 \pm 3.1$	$9.4 \pm 0.6$	$10.2 \pm 2.7$

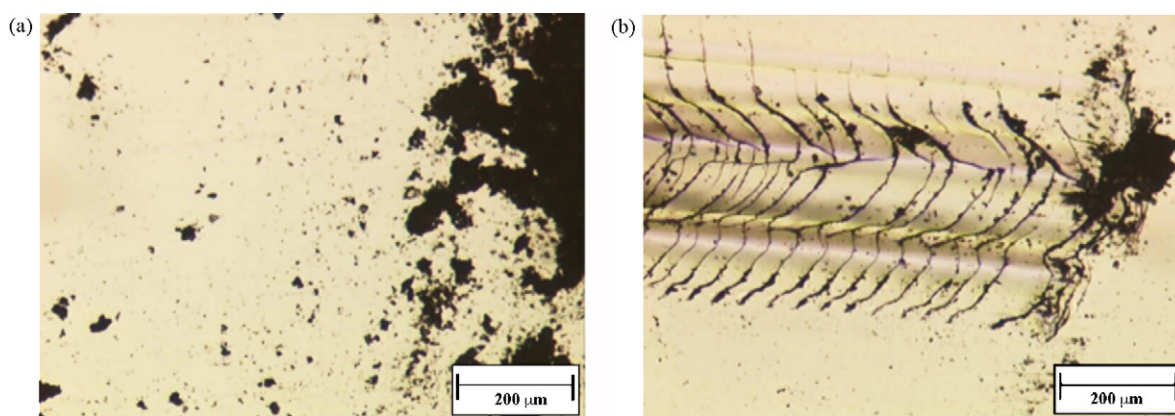
Coating thickness is within the range of  $5 \pm 0.5 \mu\text{m}$ .

Fig. 1. Micrographs of coating surfaces after pencil scratch test. The scratch direction is from right to left. (a) Soft pencil does not cause damage to the coating and (b) hard pencil causes coating cracking.

Fortunately, such effect can be incorporated into the calculation of the fracture toughness, so that the obtained values are independent material properties.

Fig. 1a shows that with softer pencil grades, there was no scratch damage to the coating. Some crumbs from the pencil lead were observed on the surface. When hard pencils were used, the coating cracked (Fig. 1b), and such damage was caused by tensile stress behind the sliding pencil lead. Film adhesion to the substrate was found to be very good in general. This could be attributed to the plasma treatment before dip coating.

The most severe damage took place when the pencil lead gouged into, and ploughed along the substrate, as shown in Fig. 2 as an example. This type of damage happened when: (1) the hardest pencil leads were used; (2) the coating was relatively thin; (3) the coating was without silica filler. Implications from the observation will be discussed later. In all the sol–gel coatings tested, the effective friction coefficient ranged from 0.27 to 0.73 when coating cracking occurred. The magnitude generally increased with increasing pencil grade. When there was no scratch damage, the friction coefficient stayed around 0.13 for all coatings. Therefore the friction coefficient might be used as an indicator for the scratch failure.

With the increase of coating thickness by multiple coating, the pencil hardness grade improved significantly. Fig. 3 shows an increase of five pencil grades from 3.8- to 25.1- $\mu\text{m}$  thick film based on a fixed colloidal silica concentration of 30.5 vol.%. A similar trend was also observed in specimens with other colloidal silica content, but the results were not presented here.

The improvement in scratch resistance by thickening the coating is very effective, and this finding is of practical interest since the amount of silica that can be added to reinforce the matrix is limited, while thickening the coating is relatively easy and unlimited.

#### 4. Discussion

In a scratch test, a tangential friction load is added to the normal contact load. This friction traction superimposes a com-

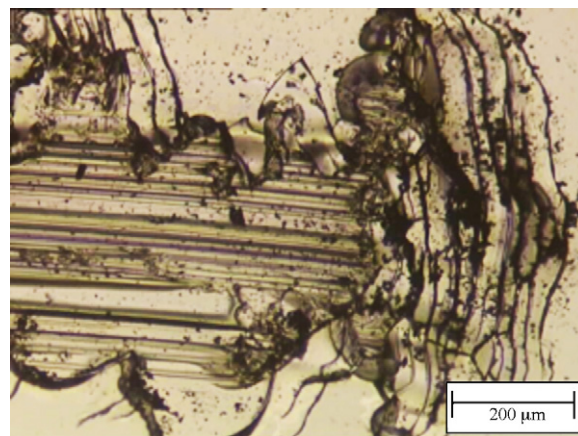


Fig. 2. Substrate gouge in a sol–gel coating without silica filler addition. The film is relatively thin and the pencil used is of the hardest grades.

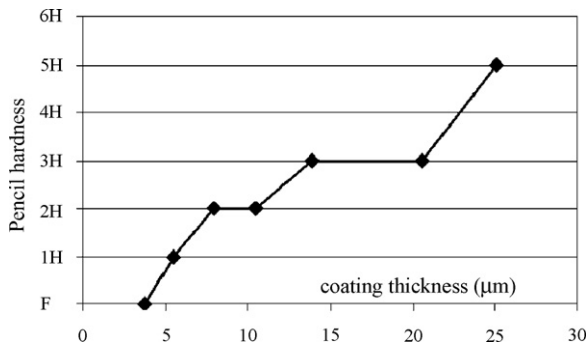


Fig. 3. Pencil hardness increases with the coating thickness. The colloidal silica content for all these specimens is 30.5 vol.%.

pressive stress at the front edge of the contact and a tensile stress to the trailing edge. Hamilton [27,28] analyzed the radial stress inside and outside a spherical stylus contact zone with different friction coefficient for a monolithic material. The maximum radial tensile stress at the trailing edge is intensified by the friction according to

$$\sigma_r^m = \frac{3P}{2\pi a^2} \left( \frac{1-2\nu}{3} + \frac{4+\nu}{8}\pi\mu \right) \quad (1)$$

in which  $P$  is the normal load (and  $P/\pi a^2$  is the average normal contact pressure for a spherical indenter),  $a$  the contact radius,  $\mu$  is the friction coefficient, and  $\nu$  is the Poisson's ratio. Meanwhile, at the front edge the tensile stress at the contact edge is reduced (by changing the “+” sign to “-” in Eq. (1)) to less tensile, or even to compressive state, depending on the friction coefficient. The maximum compressive stress occurs inside the contact zone, and the magnitude is greater than the one without friction traction. When a coating is added onto the surface of a monolithic material, the stress distribution in the coating will be similar to the one on the monolithic surface as long as the coating is thin relative to the contact radius.

In the pencil scratch tests, the contact load at the tip of the pencil was fixed at  $750 \pm 10$  g [14]. Therefore, the maximum contact stress is mainly determined by the contact area. When a flattened pencil lead was tilted at  $45^\circ$  to the coating surface (Fig. 4), the sharp tip induces a very high pressure at the point of contact. However, if the pencil lead is fragile (e.g. the one of softer pencil grades), the rupture of the pencil lead will lead to drastic increase of the contact area, and thus reduction of the contact pressure. The lead crumbs (Fig. 1a) may serve as a solid

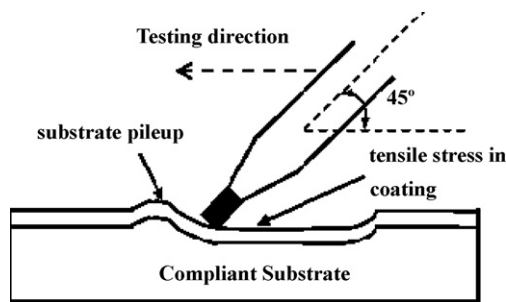


Fig. 4. Schematic response of a pencil-scratched thin film on compliant substrate.

lubricant so that when there is no damage in the coating, the measured friction coefficient stays at a low level. The tendency of crumb formation in the pencil lead of harder grades is reduced due to the increase of the clay content in the mix. Therefore, essentially the difference in using different pencil grades as the scratch stylus lays on the resulting contact pressure, and thus the magnitude of the applied stress on the coating. Compared with the conventional scratch test, where a rigid (typically diamond) stylus is used with progressively increasing normal load, pencil scratch test achieves a similar increase in the contact pressure by using progressively harder pencil leads under a fixed normal load.

The hard-grade pencil tip remains sharp so that the contact pressure is kept at a high level. In such a case, there is a high chance of severe deformation in substrate after the coating cracks. And, once the pencil tip ploughs into the substrate, the increase in the friction traction exacerbates the substrate deformation [29,30]. The hard coating can help alleviate the contact pressure on the polymer substrate so that substrate ploughing is prevented even after the coating fractures. The ability of the hard coating to spread the contact pressure is directly related to the bending stiffness of the coating, which strongly depends on its modulus and thickness. Once substrate gouging occurs, the analysis will be similar to the one for monolithic polymer scratch, which is not discussed in detail in the current work.

The schematics in Fig. 4 explains the stresses and deformation in the film-substrate system during a typical pencil scratch test. As discussed before, cracking at the trailing edge was caused by the contact action and the friction traction. Careful examination of Fig. 1b finds that the cracks are more curved along certain scratch sub-tracks, indicating strong influence from the contact stress. The less curved portions of the cracks were more influenced by the tangential friction stress. In theory, if only tangential friction stress exists, the cracks should form straight lines perpendicular to the scratch direction.

Film cracking occurs when the energy release rate reaches a critical magnitude, which is termed as the fracture toughness. The energy release rate,  $G$ , of a thin film under tensile stress for the general case of substrate yielding is given by [24,31]:

$$G = \frac{\sigma_f^2 t}{2E_f} g \left( \alpha, \beta, \frac{\sigma_f}{\sigma_y}, n \right) \quad (2)$$

where  $\sigma_f$  is the stress,  $E_f$  the modulus and  $t$  the thickness of the film. Factor  $g$  is a function of the Dundurs' parameters ( $\alpha$  and  $\beta$ , which represent the elasticity mismatch between the film and the substrate), film stress level relative to its yield strength ( $\sigma_y$ ), and the work hardening index ( $n$ ) of the substrate. During a scratch test, the tensile stress is contributed from both the contact bending and the friction traction, so that

$$\sigma_f = C_1 \frac{P}{t^2} + C_2 \frac{\mu P}{Wt} \quad (3)$$

where  $W$  is the contact width, and  $C_1$  and  $C_2$  are non-dimensional constants related to contact bending and frictional traction.

Substituting Eq. (3) into (2) and equating the energy release rate to the film fracture toughness,  $\Gamma_f$ , the critical scratch load

is given by

$$P_c = \sqrt{2tE_f\Gamma_f} \left( \frac{tW}{C_1W + C_2t\mu} \right) g \left( \alpha, \beta, \frac{\sigma_f}{\sigma_y}, n \right)^{-1/2} \quad (4)$$

It is clear that the resistance to coating cracking is adversely affected by the load (or more precisely, the pressure) and the friction coefficient. Meanwhile, it also reveals that increasing the elasticity modulus and the thickness of the coating helps reduce the tendency of the cracking driving force. Mechanically, an increase in the coating modulus and thickness translates into an increase in the stiffness of the coating; therefore the stress is reduced when other factors remain unchanged. Increasing the coating toughness surely is beneficial; however, there is a limited room for the improvement for sol–gel coatings, as illustrated in Table 2. Increasing the coating thickness can result in a remarkable improvement in the pencil hardness (Fig. 3). Increasing silica addition also improves the modulus quite significantly, and has resulted in an improvement of three pencil grades (Table 2).

The source for the tensile stress in Eq. (3) needs to be further analyzed. If the tensile trailing stress is dominated by the friction traction,  $C_2 \gg C_1$ , the critical load will be inversely proportional to the friction coefficient and square root of the thickness ( $t^{1/2}$ ). When normal contact load is the main cause for coating cracking,  $C_1 \gg C_2$ , the thickness has a greater influence ( $t^{3/2}$ ) on the critical load. This implies that increasing the thickness will be very effective in raising the critical scratch load if friction coefficient can be kept a minimum.

The influence of friction coefficient on the scratch resistance has been discussed by many other researchers [32–37]. Experimentally, various ways of achieving different friction coefficient were employed in the studies, for example, use of different indenter material, shape and diameter, deposition of a thin top layer, and application of chemical cleaning, plasma treatment, and lubricant on the coating surface.

Generally in a scratch test, film may fail by delamination driven mechanisms or film fracture-induced mechanisms [38]. In the current work, no obvious delamination failure was observed, indicating good adhesion between the film and the substrate. Nevertheless, for the completeness of the discussion, delamination driven scratch failure is briefly discussed. Bless et al. [32] found that for a sol–gel coating on polypropylene substrate, delamination-induced scratch failure could be predicted by a model similar to the one initially proposed by Evans [39]. The critical load,  $P_c$ , was given as

$$P_c = \frac{W}{v\mu} \sqrt{2tE_f\Gamma_{int}} \quad (5)$$

where  $\Gamma_{int}$  is the interfacial fracture toughness between the film and the substrate. It is noticed that this model has not considered the deformation in, and energy stored in the substrate. Therefore using this relation to predict the interfacial fracture toughness may bring in considerable error when the substrate is much more compliant than the substrate [40–42].<sup>1</sup> Nevertheless, the depen-

dence of the critical scratch failure load on the thickness ( $t$ ) and stiffness ( $E_f$ ) of the film, the friction coefficient ( $\mu$ ), and the interfacial toughness ( $\Gamma_{int}$ ) is clearly revealed. They influence the critical load in the same trend as in the case of film cracking failure.

From material point of view, two properties should be improved when designing scratch resistant brittle coatings on compliant substrate. The first is the adhesion between the coating and the substrate. Weak interface induces premature failure by delamination and spallation. Surface treatment such as plasma bombardment on the substrate can be an effective way to improve the adhesion of coatings. Interlayers have also shown a positive effect for the enhancement of interface toughness. The second is the resistance to film cracking. With sufficient interfacial toughness, coating cracking inevitably will occur with increasing load. To delay the occurrence of cracking, several possible approaches can be contemplated. (1) Since cracking is induced by the tensile stress, keeping a compressive residual stress in the coating will help counteract the tensile stress. However, the creation of compressive stress in sol–gel coating is unlikely since the coating usually shrinks after curing, leaving residual tensile stress in the coating; this may partially explain why mainly cracking, not delamination occurred in our sol–gel coatings. Therefore, effort should be made to minimize the residual tensile stress in sol–gel coatings. (2) Effective friction coefficient can be reduced by appropriate surface treatment. Reduction of the surface asperity will also be effective. Lubrication, if allowed, would certainly reduce the traction stress. (3) Coating thickness should be increased within the limit of its functional and processing constraints. For a fixed magnitude of load, a thick coating increases the stiffness and reduces the maximum stress of the coating, and thus the risk of cracking.

## 5. Conclusion

The pencil scratch resistance of sol–gel coatings on polycarbonate substrates containing different amount of colloidal silica particles was used as an example to study the general case of scratch behavior of brittle films on compliant substrates. The failure mode of the coatings was brittle cracking at the trail end when the coating failure began to occur. When harder pencils were used, substrate gouge started to take place. Key factors influencing the scratch failure were found to be the elastic modulus, fracture toughness, and thickness of the coating material. By increasing the silica content and the thickness of the coating, the pencil hardness grade increased significantly. To prevent substrate ploughing, coating thickness and elasticity modulus have to be increased.

Based on the parametric studies, it is always desirable to reduce the friction coefficient since it contributes to both delamination-induced and cracking-induced failures. Surface treatment, reduction of surface asperity, and application of lubricant are possible ways to reduce the friction. In general, to increase the scratch resistance of thin films on compliant substrates, the elasticity modulus, thickness, fracture resistance of the film, and interfacial fracture toughness between the film and the substrate should be increased.

<sup>1</sup> Refs. [40,41] also provide a method to measure thin film delamination toughness using controlled buckling test.

## References

- [1] E. Quandt, H. Holleck, *Microsyst. Technol. Microsyst. Nanosyst.-Inform. Storage Process. Syst.* 5 (1998) 49–58.
- [2] W. Grzesik, Z.Z. Zalisz, S. Krol, P. Nieslony, *Wear* 261 (2006) 1191–1200.
- [3] P. Siemroth, J. Berthold, B. Petereit, H.H. Schneider, H. Hilgers, *Surf. Coat. Technol.* 188 (2004) 684–690.
- [4] S.V. Fortuna, Y.P. Sharkeev, A.J. Perry, J.N. Matossian, I.A. Shulepov, *Thin Solid Films* 377 (2000) 512–517.
- [5] R.J. Martin-Palma, R. Gago, V. Torres-Costa, P. Fernandez-Hidalgo, U. Kreissig, J.M.M. Duart, *Thin Solid Films* 515 (2006) 2493–2496.
- [6] H. Sein, W. Ahmed, I.U. Hassan, N. Ali, J.J. Gracio, M.J. Jackson, *J. Mater. Sci.* 37 (2002) 5057–5063.
- [7] L.Y.L. Wu, G.H. Tan, X.T. Zeng, T.H. Li, Z. Chen, *J. Sol–Gel Sci. Technol.* 38 (2006) 85–89.
- [8] L.Y.L. Wu, E. Chwa, Z. Chen, X.T. Zeng, *Thin Solid Films* 516 (2008) 1056–1062.
- [9] G. Schottner, K. Rose, U. Posset, *J. Sol–Gel Sci. Technol.* 27 (2003) 71–79.
- [10] G.M. Wu, J. Shen, T.H. Yang, B. Zhou, J. Wang, *J. Mater. Sci. Technol.* 19 (2003) 299–302.
- [11] ASTM C 1624 – 05, Standard Test Method for Adhesion Strength and Mechanical Failure Modes of Ceramic Coatings by Quantitative Single Point Scratch Testing, ASTM International, 2005.
- [12] ASTM D 7027 – 05, Standard Test Method for Evaluation of Scratch Resistance of Polymeric Coatings and Plastics Using an Instrumented Scratch Machine, ASTM International, 2005.
- [13] ASTM D 7187 – 05, Standard Test Method for Measuring Mechanistic Aspects of Scratch/Mar Behavior of Paint Coatings by Nano-scratching, ASTM International, 2005.
- [14] ISO 15184:1998, Paints and Varnishes: Determination of Film Hardness by Pencil Test, ISO, 1998.
- [15] ASTM D 3363 – 00, Standard Test Method for Film Hardness by Pencil Test, ASTM International, 2000.
- [16] N. Al-Dahoudi, M.A. Aegerter, *Mol. Cryst. Liq. Cryst.* 374 (2002) 91–100.
- [17] V. Kumar, Y.K. Bhardwaj, S. Sabharwal, *Prog. Org. Coat.* 55 (2006) 316–323.
- [18] E. Chwa, L. Wu, Z. Chen, *Key Eng. Mater.* 312 (2006) 339–344.
- [19] Y.S. Lin, C.L. Chen, *Plasma Process. Polym.* 3 (2006) 650–660.
- [20] M.W. Daniels, L.F. Francis, *J. Colloids. Interf. Sci.* 205 (1998) 191–200.
- [21] H.C. Ong, R.P.H. Chang, N. Baker, W.C. Oliver, *Surf. Coat. Technol.* 89 (1997) 38–46.
- [22] Z. Chen, B. Cotterell, W. Wang, E. Guenther, S.J. Chua, *Thin Solid Films* 394 (2001) 202–206.
- [23] Z. Chen, B. Cotterell, W. Wang, *Eng. Fract. Mech.* 69 (2002) 597–603.
- [24] Z. Chen, Z. Gan, *Thin Solid Films* 515 (2007) 3305–3309.
- [25] Z. Chen, X. Xu, C.C. Wong, S. Mhaisalkar, *Surf. Coat. Technol.* 167 (2003) 170–176.
- [26] M. Nogami, Y. Moriya, *J. Non-Cryst. Solids* 37 (1980) 191–201.
- [27] G.M. Hamilton, *J. Appl. Mech.* 33 (1966) 371–376.
- [28] G.M. Hamilton, *Proc. Inst. Mech. Eng. C: J. Mech. Eng. Sci.* 197 (1983) 53–59.
- [29] R.D. Arnell, *Surf. Coat. Technol.* 43–44 (1990) 674–687.
- [30] H. Djabella, R.D. Arnell, *Thin Solid Films* 223 (1993) 87–97.
- [31] J.L. Beuth, N.W. Klingbeil, *J. Mech. Phys. Solids* 44 (1996) 1411–1428.
- [32] M.H. Brees, G.B. Winkelman, A.R. Balkenende, J.M.L. Den Toonder, *Thin Solid Films* 359 (2000) 1–13.
- [33] P.A. Steinmann, Y. Tandy, H.E. Hintermann, *Thin Solid Films* 154 (1987) 333–349.
- [34] J. Valli, *J. Vacuum Sci. Technol.* 4A (1986) 3007–3014.
- [35] S.J. Bull, D.S. Rickerby, A. Matthews, A. Leyland, A.R. Pace, J. Valli, *Surf. Coat. Technol.* 36 (1988) 503–517.
- [36] M.D.E. Coghill, D.H. St. John, *Surf. Coat. Technol.* 41 (1990) 135–146.
- [37] F. Attar, T. Johannesson, *Surf. Coat. Technol.* 78 (1996) 87–102.
- [38] Z. Chen, L.Y.L. Wu, Scratch Resistance of Protective Sol-Gel Coatings on Polymeric Substrates, Chapter 14, in: K. Friedrich, A.K. Schlarb (Eds.), *Tribology of Polymeric Nanocomposites: Friction and Wear of Bulk Materials and Coatings*, Elsevier, 2008, pp.325–353.
- [39] H.E. Evans, *Mater. High Temp.* 12 (1994) 219–227.
- [40] B. Cotterell, Z. Chen, *Int. J. Fract.* 104 (2000) 169–179.
- [41] B. Cotterell, Z. Chen, *Key Eng. Mater.* 183 (2000) 187–192.
- [42] H.H. Yu, J.W. Hutchinson, *Int. J. Fract.* 113 (2002) 39–55.